Nucleic Acids Research, 2006, Vol. 34, No. 10 ***2853–2863***
doi:10.1093/nar/gkl360

Analysis of HIV-1 replication block due to substitutions at F61 residue of reverse transcriptase reveals additional defects involving the RNase H function

Dibyakanti Mandal, Chandravanu Dash[1], Stuart F. J. Le Grice[1] and Vinayaka R. Prasad*

Department of Microbiology and Immunology, Albert Einstein College of Medicine, 1300 Morris Park Avenue, Bronx, NY 10461, USA and [1]HIV Drug Resistance Program, National Cancer Institute, Frederick, MD, USA

Received March 9, 2006; Revised March 30, 2006; Accepted April 24, 2006

ABSTRACT

We reported previously that substitutions F61L, F61W, F61Y and F61A in human immunodeficiency virus type 1 (HIV-1) reverse transcriptase affect strand displacement synthesis [T. S. Fisher, T. Darden and V. R. Prasad (2003) *J. Mol. Biol.*, 325, 443–459]. We have now determined the effect of these mutations on HIV replication. All mutant viruses were replication defective. Measuring replication intermediates in infected cells did not reveal a specific block as all mutants displayed reduced DNA synthesis (wild-type>F61L>F61W>F61Y> F61A). Analysis of 2-LTR circle junctions revealed that F61W and F61Y mutants generated increased aberrant circle junctions. Circle junctions corresponding to F61Y included 3′-PPT insertions suggesting ribonuclease H defect. *In vitro* assays mimicking PPT primer generation indicated that F61L, F61W and F61Y mutant RTs were unaffected, while F61A mutant cleaved both at PPT/U3 junction and at +6 with similar efficiencies. In assays measuring cleavage at the RNA/DNA junction to remove the PPT primer, all mutants were significantly affected with F61Y and F61A being most severely impaired. Our results show that (i) replication block of most mutants is due to more than one biochemical defect; (ii) mutations in polymerase domain can affect the function of a distal domain; and (iii) virological analyses of RT mutations can yield insight into structure–function relationship that is otherwise not obvious.

INTRODUCTION

Replication of human immunodeficiency virus type 1 (HIV-1) genome involves conversion of its RNA genome into double-stranded proviral DNA by the virion-associated RT (1). Viral reverse transcription is initiated from the cellular $tRNA^{Lys,3}$ primer that binds near the 5′ end of viral RNA at the primer-binding site. DNA synthesis proceeds to the 5′ end, forming (−) strand strong stop DNA (−ssDNA). The RNA of newly synthesized RNA–DNA hybrid is cleaved by the ribonuclease H (RNase H) activity of RT, facilitating the transfer of −ssDNA to the complementary region at the 3′ end of the genome RNA. Minus strand DNA synthesis is then continued. During this process, RNase H activity continues to degrade RNA/DNA replication intermediate, with the exception of two short, polypurine tract (PPT) sequences located at the center of the genome (cPPT) (2) and the 3′ end of the genome (3′PPT) (3). Plus strand DNA synthesis is primed from these PPTs. At the 3′ site, DNA synthesis continues until RT copies a part of tRNA molecule, which is followed by the second strand transfer and bidirectional DNA synthesis, culminating in a linear double-stranded proviral DNA with long terminal repeats (LTRs) (1).

HIV-1 RT, in addition to being a multifunctional enzyme that can carry out RNA- and DNA-dependent DNA polymerase activities and the RNase H activity, can also support strand displacement synthesis (4,5). Other retroviral RTs that have been shown to be capable of strand displacement synthesis include those of avian myeloblastosis virus (AMV) (6,7), feline immunodeficiency virus (7) and Moloney murine leukemia virus (8). Although accessory proteins, such as *Escherichia coli* single-stranded DNA-binding protein, eukaryotic replication protein A (RP-A) and HIV-1 nucleocapsid (NC) enhance strand displacement synthesis *in vitro*, RT is capable of catalyzing strand displacement synthesis in their

*To whom correspondence should be addressed. Tel: +1 718 430 2517; Fax: +1 718 430 8976; Email: prasad@aecom.yu.edu

© The Author 2006. Published by Oxford University Press. All rights reserved.

The online version of this article has been published under an open access model. Users are entitled to use, reproduce, disseminate, or display the open access version of this article for non-commercial purposes provided that: the original authorship is properly and fully attributed; the Journal and Oxford University Press are attributed as the original place of publication with the correct citation details given; if an article is subsequently reproduced or disseminated not in its entirety but only in part or as a derivative work this must be clearly indicated. For commercial re-use, please contact journals.permissions@oxfordjournals.org

absence (9–11). Two key steps in the viral life cycle involve strand displacement synthesis. The first of these occurs after second strand transfer, when minus strand DNA forms a circular intermediate via complementary sequences in the primer-binding site region. Complete synthesis of the minus-strand 5′-LTR and linearization of the intermediate requires that RT displaces ~600 nt of DNA (1). Second, the formation of central DNA flap, a *cis*-determinant of HIV-1 nuclear import, requires displacement of ~100 nt near the center of the proviral DNA (12,13).

Structure–function relationships of HIV RT are a subject of intensive investigation both due to its central role in virus replication and its importance as an antiviral target. Investigations to identify RT structural determinants of strand displacement synthesis are lacking. One study investigating interactions between RT and the duplex ahead of the active site by DNase I footprinting (14) found that the non-template strand is protected, at as far as 9 nt ahead of the catalytic center. Using RT bound to a strand displacement substrate, the 2 bp immediately in front of the enzyme were found to be melted (14). These findings suggest that RT plays an active role in unpairing the DNA ahead of polymerase active site. In a separate study from our laboratory previously, we showed that residue F61 in the fingers subdomain of HIV-1 RT p66 plays an important role in strand displacement synthesis (15). Substituting F61 with Tyr or Leu increased the efficiency of strand displacement synthesis, while a change to Trp significantly reduced this activity. These substitutions also affected processivity of polymerization by RT, but the changes in strand displacement synthesis did not correlate to those in processivity. The crystal structure of a ternary complex of HIV-1 RT (16) shows that F61 contacts a base on the single-stranded template overhang immediately 5′ of the templating base. In order to gain mechanistic insight into the role of F61 in strand displacement synthesis, a 5 bp duplex DNA was modeled, into the above structure, ahead of the active site (15). In this model, F61 residue contacts the terminal basepair of the duplex to be melted and stabilizes it to a certain degree. Replacing F61 residue with other amino acids in this structure revealed a negative correlation between the ability of the amino acid at this position to stabilize the terminal base pair and strand displacement synthesis by the corresponding mutant RT. In other words, substitutions with maximal stabilization, such as F61W led to minimal strand displacement, while those that did not stabilize the terminal base pair ahead of the active site were maximally active in strand displacement synthesis (e.g. F61L and F61Y). Thus, the F61 residue acts as a 'switch' to initiate melting of the duplex. Winshell *et al*. (17) have examined the most severely affected mutant in this set, F61W, for its effect on the melting of the +2 and +3 using the permanganate sensitivity assay. Those studies indeed confirm that F61W mutant is deficient in melting the two bases ahead of the active site (17).

In the present study, we have investigated the effect of substitutions F61L, F61W, F61Y and F61A on HIV replication. Our results indicate that all F61 mutant viruses are replication defective. Interestingly, the relative degrees of replication defects did not directly correlate to effects of the mutations on *in vitro* polymerase function of RT. Thus, the replication block in F61 substitution mutants appears to be due to additional defects in other steps of viral replication. Since the formation of 5′-LTR is accomplished via strand displacement synthesis, we analyzed 2-LTR circle junctions, as surrogate for linear viral DNA, from cells infected with the wild-type, F61L, F61W and F61Y mutants. This analysis revealed that the defects in strand displacement synthesis were partly commensurate with replication defects, but also suggested that some mutants may be defective for PPT primer removal. *In vitro* studies were performed to evaluate whether recombinant mutant RTs display RNase H defects, which showed that F61Y RT was indeed defective in RNase H-mediated removal of PPT RNA from plus DNA, while F61A was defective for both the generation of PPT RNA primer and its removal. Thus, mutations at F61, a residue contacting the incoming template strand, appear to disrupt viral replication not only due to defects in the polymerase domain function, but also in the function of the distally located RNase H domain.

MATERIALS AND METHODS

Plasmids

Mutations were introduced at the F61 residue in the HIV-1 RT of HxB2 full-length molecular clone (R3B) via cassette mutagenesis (18). In short, an intermediate molecular clone was constructed by ligating a 4.2 kb SpeI/SalI fragment spanning *gag* p24 to integrase of HIV-1 (nt 1560–5720) into pBSKS(+) vector. Using the intermediate clone as template, a 1.2 kb upstream fragment was amplified with the primers 'BS Forward' (5′-TGTAAAACGACGGCCAGTGAG-3′) and 'F61BsmB-1' (5′-CTGCAGCGTCTCCTGGAGTATTG-TATGGAT-3′). Similarly a downstream 3.0 kb fragment was amplified using the primers 'BS Reverse' (5′-GGAAACA-GCTATGACCATGAT-3′) and 'F61BsmB-2' (5′-CTGCA-GCGTCTCAGAACTTAATAAGAGAAC-3′). PCR products were digested with SpeI and PstI or SalI and PstI, respectively, and the fragments cloned into SpeI and SalI sites of plasmid pBSKS(+) via a 3-piece ligation, to generate a cassette acceptor plasmid. The cassette acceptor clone was sequenced to confirm the absence of undesired mutations, digested with BsmBI, a type II restriction enzyme followed by ligation of double-stranded adapters containing desired mutant sequences for F61 (19). The 4.2 kb SpeI to SalI fragments from the intermediate clones with each of the F61 substitutions were cloned between the SpeI and SalI sites of HIV-1_{R3B} molecular clone.

Oligodeoxyribonucleotides and oligoribonucleotides

A 40 nt oligomer containing the (+) strand DNA of HIV-1 PPT was purchased from Integrated DNA Technology (Coralville, IA). A complementary 30 nt RNA containing the HIV-1 3′ PPT and a 20 nt chimera containing 15 nt PPT RNA and 5 nt DNA from the flanking U3 sequence was purchased from Dharmacon Research (Boulder, CO). Oligonucleotides were purified by preparative PAGE and quantified spectrophotometrically (260 nm), assuming a molar extinction coefficient equal to the sum of the constituent deoxynucleotides. Hybrids were prepared by heating a 1.5:1 RNA–DNA mixture to 95°C in 10 mM Tris–HCl, pH 7.8,

25 mM NaCl for 5 min, followed by slow-cooling to 4°C. Samples were stored at −20°C.

Viruses

Mutant viruses were generated by transfecting full-length molecular clones into 293T cells. The 293T cells were maintained in DMEM containing 10% fetal bovine serum (FBS). Ten micrograms each of wild-type (HIV-1_{R3B}) and F61 mutant DNA were used. Transfection was via $CaPO_4$ procedure (Specialty Media, Phillipsburg, NJ). Ten 100 mm dishes containing ~50% confluent 293T cells were transfected with 10 μg DNA/plate of the molecular clones of wild-type or F61 mutants. Twenty-four hours after transfection, supernatants were collected, filtered through 0.45 μm filter (Costar, Corning, NY) and virus particles in the supernatant concentrated by sucrose density centrifugation using 20% sucrose. After centrifugation, the virus pellet was washed once with phosphate-buffered saline (PBS) carefully and re-suspended in PBS.

Determination of virus production and infectivity assay

Virus production after transfection was monitored by Gag p24 production using a commercially available kit (Perkin-Elmer, Boston, MA). To quantitate the infectivity of wild-type and mutant virus particles, reporter cells with lentiviral *tat*-driven expression of luciferase [CEM-LuSIV cells (20)] or β-galactosidase [P4-HeLa cells (21)] were used. Equal amounts of viruses (50 ng of p24) were used to infect CEM-LuSIV cells. Twenty-four hours after infection, cell lysates were assayed for luciferase activity (Promega, Madison, WI), measuring the output expressed as relative light units (RLUs) on a luminometer. P4-HeLa reporter cells, which contain an integrated copy of HIV LTR-driven *LacZ* gene, were used to calculate the viral titer as follows. Wild-type and F61 mutant viruses equivalent to 10 ng of p24 were used to infect P4-HeLa cells and 36 h post-infection, cells were fixed in 0.1% glutaraldehyde and stained with X-Gal (5-bromo-4-chloro-3-indolyl-β-D-galactopyranoside) to detect cells that displayed HIV infection-mediated activation of the β-galactosidase gene.

Western blot analysis of virion proteins

Virus supernatants of wild-type and F61 mutants each containing equivalent amounts of Gag p24 (~50 ng) were separately mixed with 0.5 ml 30% PEG containing 0.4 M NaCl to a final volume of 1.5 ml. The mixture was incubated overnight at 4°C and then centrifuged at 4°C for 45 min at 8000 r.p.m. (6800 *g*). The virus pellet was washed with PBS once and lysed in virus lysis buffer (50 mM Tris–HCl, pH 7.4, 100 mM DTT, 50 mM KCl, 0.025 Triton X-100 and 2% SDS). The lysate was analyzed for virion proteins by electrophoresis through a 4–20% gradient SDS–polyacrylamide gel overnight at 50 V. Proteins were transferred to nitrocellulose membrane in a *trans*-blot apparatus (Bio-Rad) and detected by immunoblotting using HIV-1-positive human sera (obtained through the NIH AIDS Research and Reference Reagent Program, Division of AIDS, NIAID, NIH: HIV-IG from NABI and NHLBI) as primary antibodies and horseradish peroxide-conjugated goat anti-human IgG as secondary antibodies. Finally, the antibody-reactive proteins were visualized by chemiluminisence using Luminol substrate (Perkin Elmer).

Multi-day replication assay

Jurkat cells were infected with wild-type and mutant viruses at similar virus-to-cell ratios (10 ng p24). Infection was carried out in 2 ml of serum-free RPMI media for 2 h at 37°C. After 2 h incubation, cells were centrifuged, washed with PBS and re-suspended in 10% FBS containing media. An aliquot of supernatant was collected from wild-type and F61 mutant virus cultures at 4-day intervals and preserved in presence of 1% Triton X-100. Gag p24 was measured as described above.

Real-time PCR quantification of reverse transcription intermediates

The specific DNA copy numbers of reverse transcription intermediates synthesized within the wild-type and F61 mutant virus-infected cells were measured by real-time PCR as described previously (22) using Taqman technology (Applied Biosystems). The primers and probes specific for (−) strand ssDNA, Gag full-length genome and 2-LTR circles were as described previously (22,23). Real-time PCR was performed on an ABI7700 apparatus (Applied Biosystems) in a final volume of 35 μl. Jurkat cells were infected with 60 ng (p24) each of wild-type and F61 mutant viruses over a period of 2 h in serum-free medium. To each well, DNase I (10 U/ml) was added (to remove carry-over viral DNA added in transfection) in presence of 10 mg/ml $MgCl_2$ and the cells were incubated for another 30 min at 37°C. Cells were washed in PBS and re-suspended in fresh media containing FBS. After 2, 24 and 48 h, respectively, cells were harvested and total DNA was isolated using Qiagen DNeasy tissue kit (Qiagen). Approximately 500 ng DNA was used for each PCR. Plasmid DNA of molecular clone, HIV-1_{R3B}, was used as reference DNA to prepare a standard curve. For the standard curve of 2-LTR circles, the 2-LTR junction sequence was PCR amplified from wild-type HIV-infected Jurkat cells and the PCR product cloned into the TA cloning vector pCR 2.1 (Invitrogen) to generate p2-LTR. The sequence of the clone was verified using the published sequence for HIV-1_{HXB2}. Dilutions of this plasmid were used to generate standard curve for 2-LTR circle DNA.

Analysis of 2-LTR circle junction sequences

The 2-LTR circle junctions were PCR amplified from wild-type and F61 mutant virus-infected Jurkat cells. Forty-eight hours post-infection, cells were washed twice with PBS and the total DNA isolated from cells using a Qiagen DNeasy tissue kit following manufacturer's protocol. Circle junction sequences were PCR amplified by a two-step nested PCR using 2-LTR circle junction specific primers as described by Julias *et al*. (22). The PCR products were analyzed on an agarose gel to detect the expected 200 bp fragment, and subsequently cloned into a TA cloning vector according to the manufacturer's protocol. Sequence determination for an average of 25 clones for wild-type and each F61 mutant was performed. Statistical analysis was performed with the 2-LTR circle junction sequences to determine the significance of differences. The data were analyzed by contingency table

analysis. Subsets of pertinent groupings were followed up with traditional two-by-two Fisher's exact tests.

RNase H assays

PPT selection was evaluated using recombinant wild-type and F61 mutant HIV-1 RT and the previously described RNA/DNA hybrids. 5′-End-labeling of the PPT-containing 30mer RNA or 20mer RNA–DNA chimera was performed with T4 polynucleotide kinase and [γ-^{32}P]ATP. Substrates were generated by annealing the radiolabeled PPT-containing RNA oligomer or RNA–DNA chimera to the 40 nt DNA. Hydrolysis was initiated by adding the wild-type or mutant enzymes to the hybrids in 50 mM Tris–HCl (pH 7.8), 50 mM NaCl, 5 mM DTT and 5 mM $MgCl_2$ at 37°C, with enzyme and substrate present at final concentrations of 15 and 50 nM, respectively. Reactions were terminated at times specified, by adding an equal volume of a formamide-based gel-loading buffer [95% (v/v) formamide containing 0.1% (w/v) bromophenol blue and xylene cyanol], and the hydrolysis products fractionated by high-voltage electrophoresis through 15% (w/v) polyacrylamide gels containing 7 M urea. Products were visualized by autoradiography and/or phosphorimaging and quantified using Quantity One software (Bio-Rad).

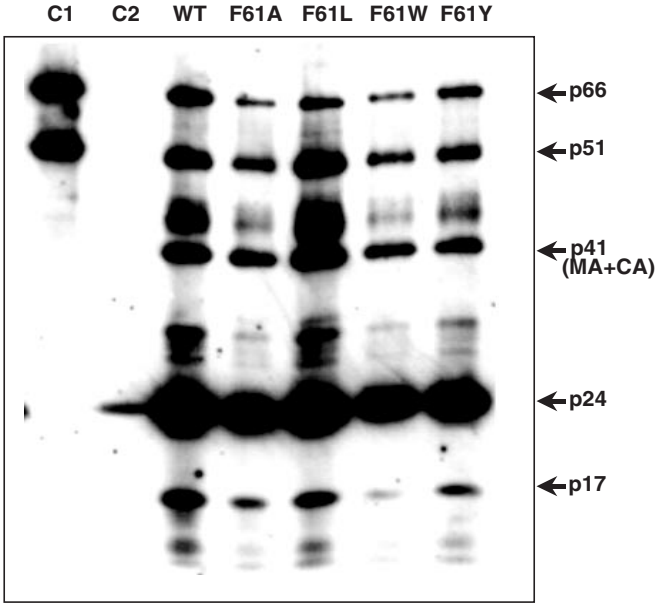

Figure 1. Analysis of wild-type and F61 mutant virion proteins. Virion proteins were isolated from wild-type and mutant viruses and resolved by electrophoresis through a 4–20% gradient SDS–polyacrylamide gel. Proteins were immunoblotted with anti-HIV antiserum (NIH AIDS Reference Reagent Program). Lanes C1 and C2 refer to positive controls, recombinant HIV-1 RT (heterodimeric with p66 and p51 bands) and p24, respectively.

RESULTS

The effect of F61 mutations on viral replication

In order to evaluate the influence of F61 substitutions (F61L, F61W, F61Y and F61A) on HIV replication, molecular clones bearing these mutations were constructed to generate virus particles. At 24 h post transfection, Gag p24 was measured in the supernatants of 293T cells transfected with these clones. Virus production by all F61 mutants was comparable to wild type (data not shown). In order to examine the effect of F61 mutation on maturation and assembly of virion proteins, lysates were subjected to immunoblot analysis. No qualitative differences in the virion protein profiles between the wild-type and the F61 mutant viruses were observed. Mutant virion particles contained correctly sized Gag p24, p66 and p51 RT proteins (Figure 1). These results indicate that F61 substitutions do not affect virion production and viral protein assembly steps of HIV replication.

In order to delineate defects in early replication events, the infectivity of wild-type and F61 mutant viruses was assayed on CEM-LuSIV cells, containing the LTR-luciferase reporter, and Hela-P4 cells containing LTR-β-gal reporter genes. The luciferase and β-galactosidase proteins are induced by the newly synthesized HIV-1 Tat protein upon infection with HIV-1. All F61 mutant viruses displayed reduced infectivity on both LuSIV and Hela-P4 cells. The infectivity of F61 mutant viruses, as assayed on LuSIV cells are shown in Figure 2A. F61A virus was non-infectious, while the infectivity of F61L, F61W and F61Y were 8.5, 2.5 and 0.6% that of wild type (Figure 2A). Our results suggest that the F61 mutant viruses have defect(s) in one or more steps during viral replication including reverse transcription, nuclear transport, integration or expression.

We next studied the replication kinetics of wild-type and F61 mutant viruses by infecting Jurkat T cells with equal amounts (10 ng p24) of wild-type and F61 mutant viruses. We measured p24 in the supernatants collected at 4-day intervals over a period of 20 days, which showed that each of the F61 mutant viruses was unable to replicate as efficiently as wild-type virus. No p24 protein was detected in the culture supernatants of F61A and F61Y viruses. Highest p24 production by wild-type virus was observed at day 8. At day 8, the average p24 value of wild type was 1040 ng/ml and F61L and F61W produced only 72 and 10 ng/ml of p24 (Figure 2B and inset within this figure). Both F61A and F61Y failed to produce any detectable amounts of p24 protein. Among the four F61 mutants, F61L displayed some replication capability although it was at least 14 times less than the wild type (Figure 2B) at peak level. F61W was also replication defective with very low amount of p24 production through 20 days. The slow replication of F61W mutant is in partial agreement with a previous study, in which the F61W mutant virus displayed delayed replication kinetics (24).

Analysis of intracellular reverse transcription to detect specific blocks

It was of interest to define the specific step in viral replication that is affected by the F61 mutations. The progress of retroviral reverse transcription process can be monitored via PCR using primers designed to detect specific replication intermediates. In order to quantify the intermediates synthesized by wild-type and F61 mutants, we carried out real-time PCR at 2, 24 and 48 h post infection, using primers and probes specific for (i) the −ssDNA (early reverse transcription), which

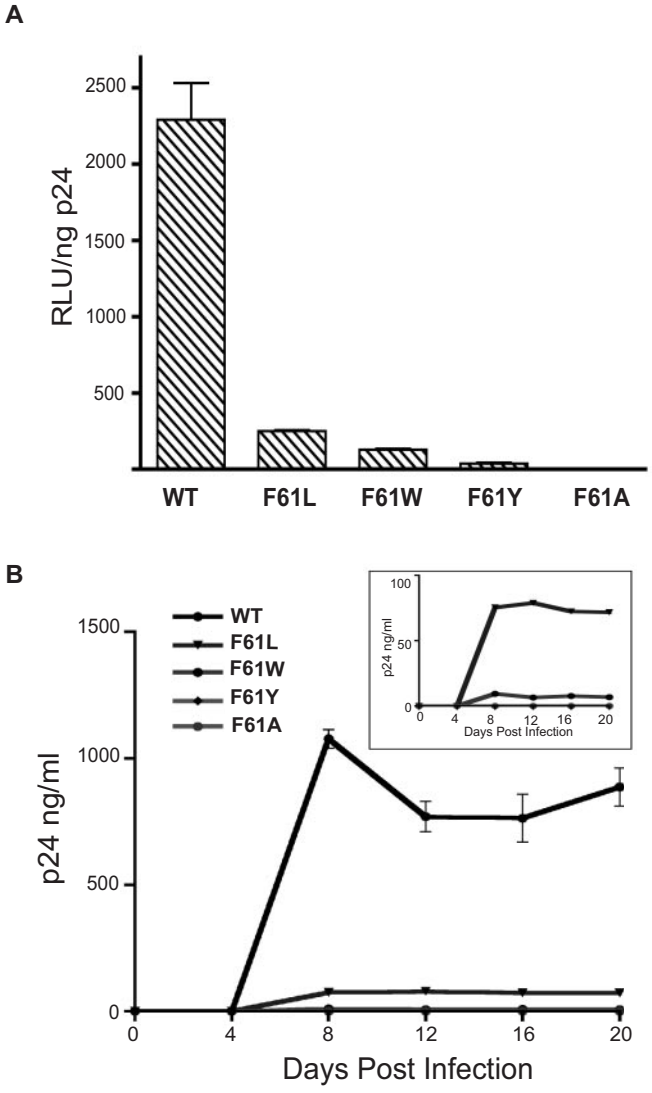

Figure 2. (**A**) Infectivity of wild-type and F61 mutant viruses. RLUs are obtained in duplicate and presented with error bars. (**B**) Replication kinetics of wild-type and F61 mutant HIV-1 viruses. Jurkat cells were infected with equal amounts of wild-type and F61 viruses, cultures maintained for 20 days and the amount of p24 produced in the supernatant measured at 4-day intervals. The inset graph depicts the data for mutant viruses alone for clarity.

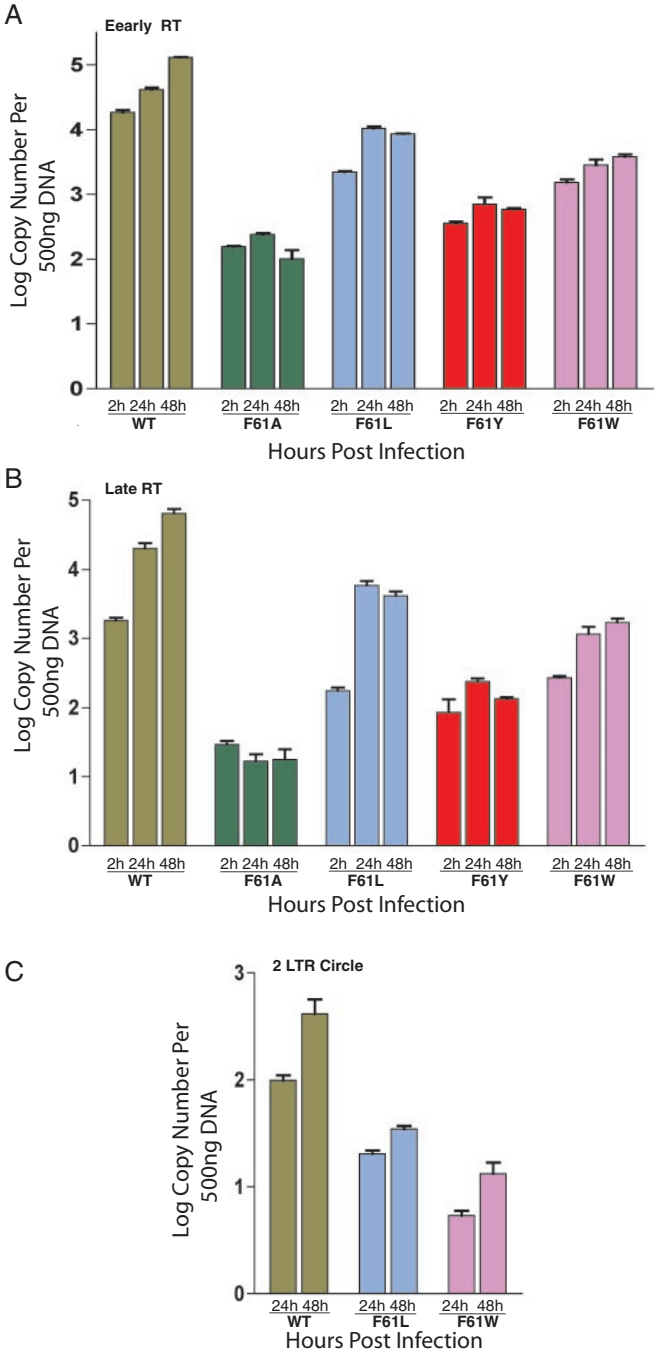

Figure 3. Real-time PCR quantification of reverse transcription products synthesized by wild-type and F61 mutant viruses in Jurkat cells at 2, 24 and 48 h. DNA copy number was quantified per 500 ng of infected cellular DNA. (**A**) Copy number of early reverse transcription product (R-U5). (**B**) DNA copy number of late reverse transcription products (*gag*). (**C**) Copy numbers of 2-LTR circle DNA.

is the earliest product of reverse transcription; (ii) gag sequences, which signify the production of full-length viral DNA (late reverse transcription); and (iii) the 2-LTR circle DNA, which indicates nuclear import of synthesized DNA.

Both early and late RT products formed by the F61 mutant viruses were reduced compared with wild-type virus at the time points tested (Figure 3). With respect to reverse transcription intermediates, no particular step appeared to be specifically affected. Rather, there was a general reduction in the viral DNA synthesis at all steps. The efficiency of −ssDNA DNA synthesis was in the order of wild-type>F61L>F61W> F61Y>F61A. However, all mutant viruses displayed consistent increase in −ssDNA synthesis from 2 to 24 h post infection (Figure 3). The F61 mutant viruses were also unable to synthesize late RT products as efficiently as wild type. At 2 h post infection, F61W was able to synthesize late RT products as efficiently as F61L. Similar to the −ssDNA, the amount of gag DNA synthesis increased from 2 to 24 h for wild-type, F61L, F61W and F61Y (Figure 3) whereas F61A failed to synthesize significant amount late RT products even at 24 h.

The 2-LTR circle DNA was not detected in wild-type or the F61 mutant virus-infected cells at 2 h post infection. For wild-type virus, this is consistent with the fact that nuclear import of reverse transcription intermediates is a late event. However, for mutants F61L and F61W, just as in the case of −ssDNA and *gag* DNA intermediates, the level of 2-LTR circle DNA was lower than wild type at 24 and 48 h post-infection, while F61A and F61Y mutants failed to make any 2-LTR circle DNA (Figure 3). At 24 h post-infection, the copy number of 2-LTR circle DNA synthesized by wild type was 95, which is ∼5 times higher than F61L and ∼16 times more than that of F61W. The amount of 2-LTR circle DNA formed by wild type, F61L and F61W increased from 24 to 48 h (Figure 3), though the level of increase was much higher for wild type. At 48 h post infection, wild-type virus was able to form 2-LTR circle DNA ∼10 and ∼27 times higher than F61L and F61W, respectively.

Sequence analysis of 2-LTR circle junction

In order to evaluate the extent of strand displacement synthesis, we directly analyzed the structure of strand displacement product (5′-LTR) synthesized during viral DNA synthesis in cells infected by F61 mutant viruses. After nuclear transport, a low, but significant proportion of the linear viral DNA is circularized. Thus, it is possible to gain an insight into the structure of both termini of the linear DNA by sequencing 2-LTR circle junctions.

We PCR amplified a 188 bp fragment around the U5–U3 junction from cells infected with wild-type, F61L, F61W and F61Y mutant viruses. A nested PCR approach allowed us to obtain products even from F61Y virus infected cells (where real-time PCR did not detect any products), but we were unable to recover any sequences for F61A mutant. Amplified DNA was cloned and ∼25 clones each for wild-type, F61L, F61W and F61Y mutant viruses were sequenced. The sequences were aligned and their LTR structures are depicted in Figure 4 (sequences themselves are included in Supplementary Data). Analysis of wild-type virus revealed that ∼40% of the clones contained the consensus 2-LTR junction sequence. A majority of the remaining sequences have either large (>100 bp) or small deletions. One sequence contained a 31 bp insertion, corresponds to the PPT and its 5′-flanking sequence (Figure 4). Among the mutants, F61L virus produced sequences with a distribution similar to wild type, with close to 50% consensus sequences. For F61W mutant virus, 40% of the sequences had either large or partial deletions (Figure 4). Seven sequences had a unique deletion at the U3 region (25%, $P < 0.02$). Interestingly, all 26 F61Y sequences had a unique 9 base insertion of 'TTAGGGGGG' sequence ($P < 0.001$; Figure 4), which corresponds, in part, to an unprocessed segment of PPT primer. The presence of only one species of sequences with unprocessed PPT suggests that the F61Y RT may be defective in its ability to remove the PPT primer RNA (also see Discussion).

Ability of F61 mutants to generate PPT primer and its removal from plus DNA

Virological analysis described above suggested a possible defect in the ability of F61Y RT-associated RNase H to efficiently remove the PPT primer from plus strand DNA. Retroviral RNase H is involved in two specific steps during initiation of plus strand DNA synthesis. First, following minus strand DNA synthesis across the PPT sequence, RNase H activity cleaves at the 3′ terminus, thereby providing a primer for plus strand, DNA-dependent DNA synthesis. Second, subsequent to the initiation of plus strand DNA synthesis the PPT RNA is removed by a cleavage at the RNA–DNA boundary. We first examined the wild-type and F61 mutant RTs for their ability to cleave a PPT-containing 30 nt oligoribonucleotide annealed to DNA. The results show that mutants F61L, F61W and F61Y display mild reductions in cleavage at position −1 (Figure 5A and B and Table 1) with efficiencies of cleavage being 77, 68 and 50% of wild type (at 3 min). The F61A RT mutant was most compromised with 6% cleavage efficiency compared to wild-type HIV-1 RT. Interestingly, F61A mutant also displayed enhanced cleavage at +6 position of the U3. Using 3′ end-labeled substrates, we showed previously that PPT-containing RNA/DNA hybrids were cleaved at the PPT/U3 junction and position +6 with almost equal efficiency (25). In keeping with data from Champoux and co-workers (26), this dual cleavage event and dissociation of the resulting hexanucleotide has been proposed as a means of providing a short single-stranded template overhang to assist initiation of plus strand DNA synthesis.

We next tested the ability of wild-type and mutant RTs to cleave at the same site, but this time using substrate with a PPT-containing RNA/DNA hybrid at the PPT/U3 junction (defined as position −1 in Figure 5A). Cleavage at the RNA–DNA junction in this substrate mimics removal of the PPT primer from nascent plus strand DNA to create properly processed U3 LTR terminus. Figure 5D shows a time course of the cleavage reactions using this substrate. Correct cleavage to remove the PPT primer occurs at the RNA/DNA junction as shown (Figure 5D, wild type). Mutants F61L, F61W and F61Y all show significant cleavage at this position, but are reduced 5- to 10-fold compared with wild-type levels. Of these three RT mutants, F61Y indeed shows the lowest level of cleavage, while F61A appears to be severely compromised (Figure 5D and Table 1).

DISCUSSION

We have examined the influence of F61 substitution mutations (19), shown previously to affect strand displacement synthesis (15,17) on viral replication. None of the mutants tested (F61L, F61W, F61Y and F61A) showed specific defects in the assembly (Figure 1) or production of virion particles (data not shown). All F61 mutants were compromised for infectivity. Experiments to measure virus spread showed that mutant viruses were defective in the order of wild-type>F61L>F61W>F61Y≥F61A. Attempts to identify specific blocks to virus replication, using real-time PCR to measure reverse transcription intermediates, revealed decreased levels of both early and late reverse transcription products, which appeared to reflect a generalized defect in DNA replication process rather than a specific block in strand displacement synthesis.

Our previous *in vitro* biochemical studies with F61-substituted recombinant RT mutants provided a valuable

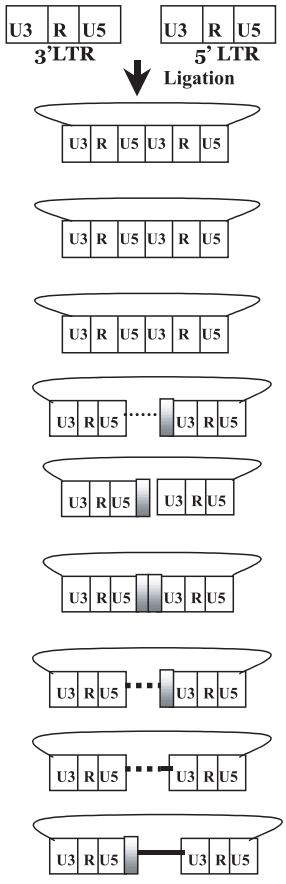

2-LTR Circle Junction	WT	F61L	F61W	F61Y
Consensus	0.39	0.50	0.36	0.00
[a]T → A Mutation at U5 edge	0.09	0.00	0.00	0.00
[b] tRNA cleavage at DNA/RNA boundary	0.09	0.14	0.00	0.00
U3 deletion + insertion of tRNA fragment	0.00	0.14	0.00	0.00
U5 deletion	0.22	0.045	0.11	0.00
U5+U3 deletion	0.17	0.23	0.29	0.00
U3 deletion + insertion of PPT & flanking sequence	0.00	0.00	0.25	0.00
Insertion of PPT + flanking Sequence	0.00	0.00	0.00	1.00
U5 deletion + insertion of PPT& flanking sequence	0.04	0.00	0.00	0.00

a. A T → A mutation in the sequence 5' CAGT 3' at the U5 edge .
b. HIV-1 RNase H normally cleaves the $tRNA^{Lys,3}$ between the two terminal ribonucleotides CA. In this case, however, the cleavage occurred between RNA/DNA boundary.

Figure 4. Summary of 2-LTR circle junction sequences from cells infected with wild-type or F61 mutant viruses. The 2-LTR circle junctions are generated by ligation of the LTR ends of full-length linear viral DNA as shown on the top left. The canonical, simple ligation of the 2-LTRs is labeled 'consensus' and shown at the top, followed by the various non-canonical forms due to improper cleavage of one of the primers, incomplete strand displacement synthesis or other causes as listed next to each diagram. PPT insertions are represented as solid lines, sequences from upstream of PPT as square dots, tRNA insertions as dots and deletions within the U5 or U3 as gray boxes. The fraction of each type of 2-LTR circle junction generated by wild-type and F61 mutant viruses are presented in the table. The box at the bottom lists the percentage of intact, fully formed U3 sequences for each virus.

yardstick to understand the viral replication defects (19). However, it must be pointed out that those studies employed subunit-selective mutagenesis such that only the p66 subunit contained the substitution, while the p51 was wild type. For site-directed mutations that are not found in the clinical isolates, p66-selective mutagenesis is the preferred approach as it minimizes possible heterodimer instability via the mutation in the p51 subunit. Viruses employed here, however, contained RT heterodimers with the mutation on both subunits. We feel that the virological effects obtained do not indicate dimerization defects, although some effect on heterodimer stability cannot be ruled out.

The extent of intracellular reverse transcription correlated well with infectivity and replication capacity of mutant viruses (Table 1 and Figure 2). Quantitative data on the intracellular reverse transcription also provided us an opportunity to compare it with our previous *in vitro* studies on RT function (15,19). Those studies showed that recombinant RTs with substitutions F61L, F61W and F61Y displayed wild type or higher levels of RNA-dependent DNA polymerase activity, while F61A RT displayed a decrease. In addition, the F61Y, F61L and F61A RTs exhibited lowered processivity (in that order) while F61W mutant RT displayed higher processivity compared with wild type (15). On the other hand, the F61L and F61Y mutant RTs had much higher strand displacement activity than wild-type RT *in vitro*. Thus, it is understandable that despite a lower processivity of RT mutant F61L (15) (Table 1), the generally more robust RT activity including strand displacement synthesis may support efficient elongation during viral DNA synthesis, permitting a basal virus replication and a minimally affected intracellular viral DNA synthesis. Thus, it appears that despite the lowest processivity of all the mutants and a 5-fold reduction in one of the RNase H activities tested (PPT-primer removal) compared to wild type, the F61L virus displayed the highest replication capacity among the mutant viruses. This is interesting considering the fact that F61L is less processive than F61W. F61W RT displayed enhanced *in vitro* RT activity and

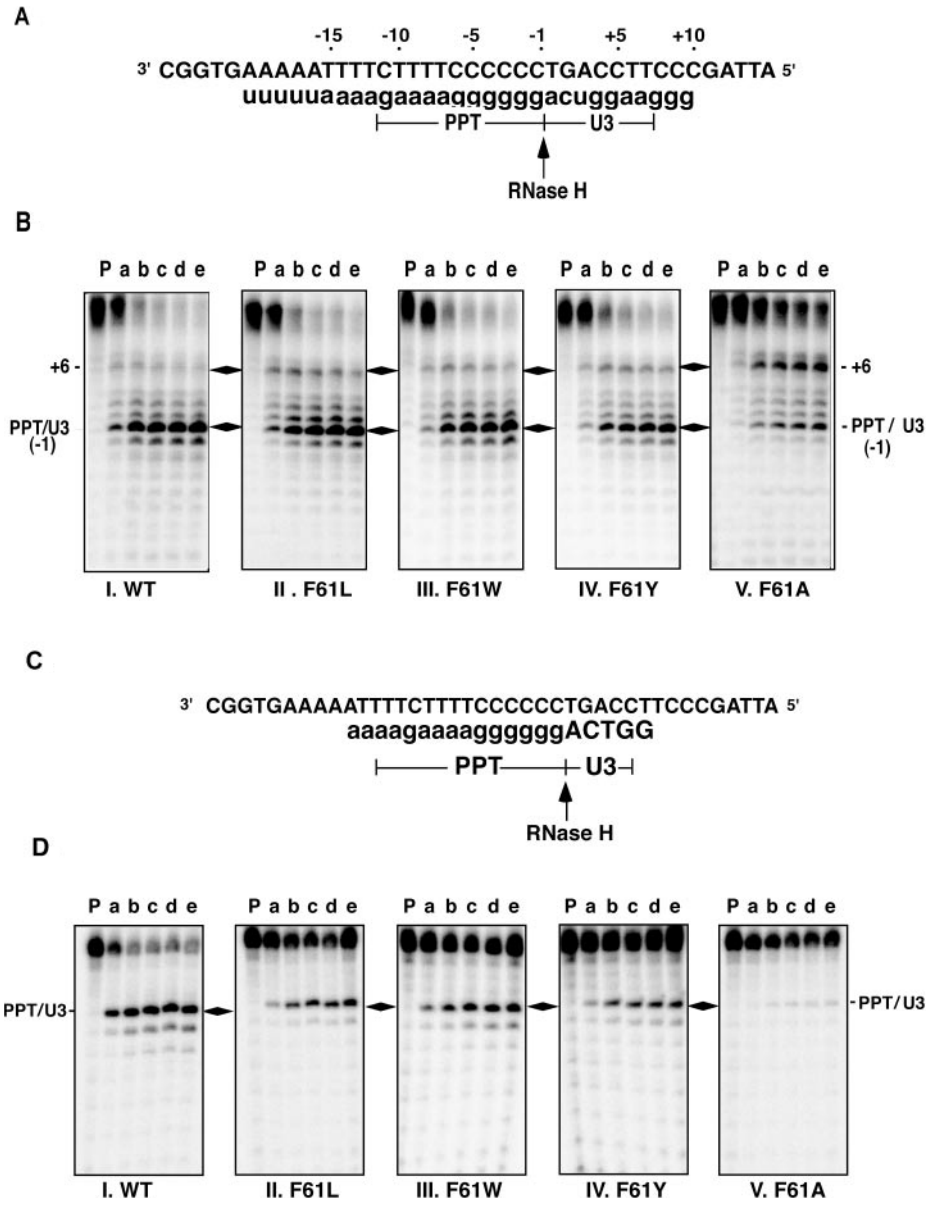

Figure 5. RNase H-mediated Polypurine tract selection. (**A**) Sequences of the oligonucleotides in the RNase H substrate for the generation of PPT primer. A 30mer plus RNA annealed to a 39mer plus DNA strand is shown. The major RNase cleavage at −1 is depicted by an arrow. Template numbering defines +5 as the fifth nucleotide downstream of the 3′ end of PPT. Numbering defines −1 as the last nucleotide of PPT RNA. RNA sequence is shown in lowercase letters and DNA sequence in uppercase. (**B**) RNase H cleavage profile of PPT/U3 RNA/DNA substrate by wild-type and F61 mutant RTs. The 5′ end labeled RNA/DNA hybrid substrates were incubated with wild type or each of F61 mutant RTs and RNase mediated hydrolysis was carried out for specified times. Hydrolysis by wild-type or F61 mutant RTs are indicated. Lanes P, a, b, c, d and e correspond to 0, 1, 3, 5, 7 and 10 min, respectively. Hydrolysis products were fractionated through 15% (w/v) polyacrylamide gels and visualized by phosphorimaging. Bands resulting from cleavages at PPT/U3 junction and +6 position are indicated on the left and right sides of panel. (**C**) A 20mer chimeric oligonucleotide containing 15mer PPT RNA attached to a pentameric oligodeoxynucleotide is annealed to 39mer minus DNA strand. (**D**) Hydrolysis pattern of a PPT/U3 specific RNA/ RNA–DNA chimera by wild-type and F61 mutant RTs. Time points for RNase-mediated cleavage are indicated. Lanes P, a, b, c, d and e correspond to 0, 1, 3, 5, 7 and 10 min, respectively. Cleavage products were analyzed as described above. Specific cleavages at U3/PPT junctions are indicated by arrows.

processivity equivalent to wild-type RT, but exhibited the lowest *in vitro* strand displacement synthesis of all mutants studied (Table 1). In fact, F61W appears to be similar to F61L in all respects except for its lowered strand displacement activity (Table 1). Among the four F61 mutant viruses studied, the F61A mutant was the least infectious, replication-defective and produced the lowest level of viral DNA and no 2-LTR circles (Figure 3). Though F61A RT had a near wild-type-like strand displacement activity, the processivity of this enzyme was severely reduced (Table 1). Thus, the replication defect of F61A virus appeared to be a combination of lower enzymatic activity and processivity. F61Y RT displayed *in vitro* polymerase and strand displacement synthesis properties exceeding those of wild-type RT and near wild-type processivity on both RNA and DNA templates. Thus, impairment of intracellular viral DNA synthesis by the

Table 1. The influence of F61 mutations on various enzymatic and virological functions

Enzyme	RDDP activity[a]	DDDP activity[a]	Processivity[b] (DDDP and RDDP)	S.D. 3′-PPT[b]	Percent normal 2-LTR junctions[c]	RNase H PPT primer generation[d] (%)	RNase H PPT primer removal[e] (%)	Infectivity[f] (percent WT)	Intracellular reverse transcription[g]
WT	+	+	+++	+	40% ($n = 23$)	100	100	100	20 300
F61L	++/+	++	+	++	50% ($n = 22$)	77	20	8.5	5840
F61W	+++	+++	++++	+/−	35% ($n = 28$)	68	19	2.5	1150
F61Y	++++	+++	++	++	0% ($n = 26$)	50	9	0.6	238
F61A	+	+/−	+/−	+	ND	6	3	ND	17

[a]Data from Fisher and Prasad (19).
[b]Data on strand displacement synthesis (S.D.) using 3′-PPT substrate from Fisher *et al*. (15).
[c]Data from the results described in Figure 4.
[d]Data from results presented in Figure 5B. Numbers correspond to −1 cleavage.
[e]Data from results presented in Figure 5D.
[f]Data from the results described in Figure 2.
[g]No. of copies of Gag-full-length DNA at 24 h from the real-time PCR results described in Figure 3.

F61Y virus could not be explained by the *in vitro* behavior of polymerase activities of F61Y mutant RT.

After completion of viral DNA synthesis in the cytoplasm, double-stranded viral DNA is imported to the nucleus, where it is integrated into the host chromosome. Unintegrated viral DNA is circularized through a variety of mechanisms (27). One form is the 2-LTR circle, which results from ligation of LTR ends of linear viral DNA. Sequence analysis of 2-LTR circle junctions, as a surrogate to determine the state of the unintegrated linear DNAs, provides valuable information on steps such as initiation of plus strand DNA synthesis, incomplete LTR formation due to impaired strand displacement synthesis and removal of tRNA or PPT primers (28). However, two caveats must first be recognized. The 2-LTR circles represent a by-product rather than an intermediate for the next step, integration. Second, the pool of 2-LTR circles is likely enriched for molecules that failed to proceed to a successful integration event. Despite these caveats, the 2-LTR circles constitute a reasonable sample of the total viral DNA synthesized and yield useful information on the status of the linear DNA precursor population. Intact U3 termini in the 2-LTR circle junctions suggest completion of strand displacement synthesis. However, deletions at the U3 termini tend to be a combination of both incomplete strand displacement and incomplete plus strand primer removal. Incomplete removal of the PPT or tRNA primer can result in single-stranded termini in the linear DNA, which trigger nucleolytic removal due to their longer half-lives (1). Despite using nested PCR, we failed to recover 2-LTR circle junctions from cells infected with F61A mutant virus, consistent with the absence of 2-LTR circles in the real-time PCR analysis (Figure 4). In contrast, circle junction sequences were recovered with mutant F61Y, which also did not show any 2-LTR circles in that analysis.

Analysis of a larger number of circle junction sequences reveals significant diversity in the types of sequences amplified, thus assuring that the products analyzed do not represent amplification of a single species. Our study shows that sequence distribution of 2-LTR circle junctions generated by wild-type virus is in agreement with the previous reports by other groups (24,28,29). The distribution of 2-LTR circles formed by the F61L mutant virus was largely similar to that of wild-type, while that of F61W and F61Y mutant viruses differed. Although F61W mutant displayed a similar proportion of consensus sequences (0.36 for F61W versus 0.39 for wild type), seven of 28 sequences (0.25) contained a unique U3 deletion and insertion of the PPT and flanking sequences (Figure 4). This suggests both incomplete strand displacement synthesis and incomplete removal of the PPT primer. The fact that F61Y virus produced very few 2-LTR circles that could not be detected by real-time PCR suggests that the sequences recovered by nested PCR are amplification of a rare event or represent multiple, identical events. In any event, the prevalence of PPT sequences suggests inefficient removal of the plus strand primer. Although the distal positioning of F61 to RNase H does not immediately suggest the influence of F61 mutations on that activity, we have studied the effect of these mutations on PPT removal using recombinant purified RTs *in vitro*.

The results of *in vitro* RNase H PPT-primer generation and primer removal assays showed that F61Y is indeed defective for PPT removal with one of lowest levels among F61 mutants (9% of wild type, Figure 5D and Table 1). Furthermore, the results of the RNase H assays highlight the following features: (i) mutating a residue that contacts the template 5′-overhang can affect the activity of a distal domain such as RNase H with an active site located ∼18 bp along the template–primer duplex; (ii) F61A RT is defective both in the efficiency and specificity of cleavage at the PPT/U3 RNA junction during generation of the PPT primer, while the ability to cleave at the PPT/U3 junction is abrogated. The RNase H defect cumulatively with other *in vitro* defects, explains the rather severe defect of this mutant; and (iii) F61Y RT is mildly affected for PPT/U3 RNA cleavage, but shows reduced cleavage at PPT/U3 RNA–DNA junction, which correlates with virological results from the 2-LTR junction sequence analysis. These results provided new insight into an additional defect of F61Y mutant that appears to have contributed to its severe replication defect.

'Long-range' effects of polymerase domain mutations such as F61Y and F61A are not without precedent and have been well documented. For example, several insertion mutations in the polymerase domain of HIV-1 RT had mild to severe effects on RNase H activity (30–32). Furthermore, site-directed mutations have demonstrated that (i) mutating W232 of the DNA polymerase primer grip (33) or deletion of a 13-residue C-terminal deletion of the non-catalytic p51 subunit (34) can modulate RNase H activity and

(ii) mutations at residues that can alter RT-template–primer interactions, can alter both the efficiency and specificity of RNase H cleavage (35). Such insights have also been obtained previously with other RT mutations. For example, Julias *et al*. (36) analyzed the 2-LTR circles from M184V and M184T mutant viruses. Although M184V mutant sequences were largely similar to those of wild type, the M184T mutant sequences included those with the insertion of tRNA in the 2-LTR junctions. This suggested a defect in the RNase H function caused by the M184T mutation.

Our results show that most F61 substitutions lead to defects in viral replication not only due to their effects on strand displacement, but also due to causes such as defects in elongation (F61L) and the efficiency and specificity of RNase H cleavages at the PPT (F61Y and F61A). We speculate that altering the contact near the template 5′-overhang can affect RNase H cleavage specificity due to a role for F61-template contact in repositioning of the enzyme during RNase H cleavage. The F61 mutations also appeared to exert their influence on viral replication partly due to a generalized reverse transcription defect that could not be predicted from the *in vitro* behavior of the mutant enzymes. As mentioned before, we do not believe that this early defect is due to an elongation defect caused by heterodimer instability. Other possible causes for an early defect could be potentially in the interaction with nucleocapsid protein or Integrase, both of which have been shown to interact with HIV-1 RT (37,38). In fact, the Integrase-interaction domain on HIV-1 RT has been mapped on to fingers-palm domains. Additional studies are needed to pinpoint the early defect of these mutants. The F61W mutant appears to suffer partly due to a strand displacement synthesis defect (as shown by greater U3 deletions and insertion of PPT sequences) since it appears equal in all other respects to F61L, which replicates much better.

SUPPLEMENTARY DATA

Supplementary Data are available at NAR Online.

ACKNOWLEDGEMENTS

The authors would like to acknowledge Ganjam V. Kalpana, Scott Garforth and Elizabeth H. Luke for critically reading the manuscript, and Albert Einstein Comprehensive Cancer Center's DNA core facility for the use of DNA sequencing services and Einstein/MMC Center for AIDS Research for the use of BL3 facility. The research described in this report was supported by a Public Health Service research grant to V.P. (NIH AI 30861) and in part by the Intramural Research Program of the NIH, NCI and Center for Cancer Research (C.D. and S.F.J.G.). Funding to pay the Open Access publication charges for this article was provided by an NIH grant (R01 AI 30861) to VRP.

Conflict of interest statement. None declared.

REFERENCES

1. Goff,S.P. (2001) Retroviridae: The Retroviruses and their replication. In Howley,P.M. and Knipe,D.M. (eds), *Field's Virology, 4th edn*. Lippincott Williams & Wilkins, Philadephia, Vol. 2, pp. 1871–1940.
2. Charneau,P., Alizon,M. and Clavel,F. (1992) A second origin of DNA plus-strand synthesis is required for optimal human immunodeficiency virus replication. *J. Virol*., **66**, 2814–2820.
3. Pullen,K.A. and Champoux,J.J. (1990) Plus-strand origin of human immunodeficiency virus type I: implications for integration. *J. Virol*., **64**, 6274–6277.
4. Huber,H.E., McCoy,J.M., Seehra,J.S. and Richardson,C.C. (1989) Human Immunodeficiency Virus 1 reverse transcriptase: template binding, processivity, strand displacement synthesis, and template switching. *J. Biol. Chem*., **264**, 4669–4678.
5. Hottiger,M., Podust,V.N., Thimmig,R.L., McHenry,C. and Hubscher,U. (1994) Strand displacement activity of the human immunodeficiency virus type 1 reverse transcriptase heterodimer and its individual subunits. *J. Biol. Chem*., **269**, 986–991.
6. Boone,L.R. and Skalka,A.M. (1981) Viral DNA synthesized *in vitro* by avian retrovirus particles permeabilized with melittin. II. Evidence for a strand displacement mechanism in plus-strand synthesis. *J. Virol*., **37**, 117–126.
7. Matson,S.W., Fay,P.J. and Bambara,R.A. (1980) Mechanism of inhibition of the avian myeloblastosis virus deoxyribonucleic acid polymerase by adriamycin. *Biochemistry*, **19**, 2089–2096.
8. Whiting,S.H. and Champoux,J.J. (1994) Strand displacement synthesis capability of Moloney murine leukemia virus reverse transcriptase. *J. Virol*., **68**, 4747–4758.
9. Kelleher,C.D. and Champoux,J.J. (1998) Characterization of RNA strand displacement synthesis by Moloney murine leukemia virus reverse transcriptase. *J. Biol. Chem*., **273**, 9976.
10. Fuentes,G.M., Rodriguez-Rodriguez,L., Palaniappan,C., Fay,P.J. and Bambara,R.A. (1996) Strand displacement synthesis of the long terminal repeats by HIV reverse transcriptase. *J. Biol. Chem*., **271**, 1966–1971.
11. Amacker,M., Hottiger,M., Mossi,R. and Hubscher,U. (1997) HIV-1 nucleocapsid protein and replication protein A influence the strand displacement DNA synthesis of lentiviral reverse transcriptase. *AIDS*, **11**, 534–536.
12. Zennou,V., Petit,C., Guetard,D., Nerhbass,U., Montagnier,L. and Charneau,P. (2000) HIV-1 genome nuclear import is mediated by a central DNA flap. *Cell*, **101**, 173–185.
13. Charneau,P., Mirambeau,G., Roux,P., Paulous,S., Buc,H. and Clavel,F. (1994) HIV-1 reverse transcription: a termination step at the center of the genome. *J. Mol. Biol*., **241**, 651–662.
14. Winshell,J. and Champoux,J.J. (2001) Structural alterations in the DNA ahead of the primer terminus during displacement synthesis by reverse transcriptases. *J. Mol. Biol*., **306**, 931–943.
15. Fisher,T.S., Darden,T. and Prasad,V.R. (2003) Substitutions at Phe61 in the beta3–beta4 hairpin of HIV-1 reverse transcriptase reveal a role for the Fingers subdomain in strand displacement DNA synthesis. *J. Mol. Biol*., **325**, 443–459.
16. Huang,H., Chopra,R., Verdine,G.L. and Harrison,S.C. (1998) Structure of a covalently trapped catalytic complex of HIV-1 reverse transcriptase: implications for drug resistance. *Science*, **282**, 1669–1675.
17. Winshell,J., Paulson,B.A., Buelow,B.D. and Champoux,J.J. (2004) Requirements for DNA unpairing during displacement synthesis by HIV-1 reverse transcriptase. *J. Biol. Chem*., **279**, 52924–52933.
18. Boyer,P.L., Ferris,A.L. and Hughes,S.H. (1992) Casette mutagenesis of the reverse transcriptase of human immunodeficiency virus type 1. *J. Virol*., **66**, 1031–1039.
19. Fisher,T.S. and Prasad,V.R. (2002) Substitutions of Phe61 located in the vicinity of template 5′-overhang influence polymerase fidelity and nucleoside analog sensitivity of HIV-1 reverse transcriptase. *J. Biol. Chem*., **277**, 22345–22352.
20. Roos,J.W., Maughan,M.F., Liao,Z., Hildreth,J.E. and Clements,J.E. (2000) LuSIV cells: a reporter cell line for the detection and quantitation of a single cycle of HIV and SIV replication. *Virology*, **273**, 307–315.
21. Kimpton,J. and Emerman,M. (1992) Detection of replication-competent and pseudotyped human immunodeficiency virus with a sensitive cell line on the basis of activation of an integrated beta-galactosidase gene. *J. Virol*., **66**, 2232–2239.
22. Julias,J.G., Ferris,A.L., Boyer,P.L. and Hughes,S.H. (2001) Replication of phenotypically mixed human immunodeficiency virus type 1 virions containing catalytically active and catalytically inactive reverse transcriptase. *J. Virol*., **75**, 6537–6546.

23. Butler,S.L., Hansen,M.S. and Bushman,F.D. (2001) A quantitative assay for HIV DNA integration *in vivo*. *Nature Med.*, **7**, 631–634.
24. Svarovskaia,E.S., Barr,R., Zhang,X., Pais,G.C., Marchand,C., Pommier,Y., Burke,T.R.,Jr and , Pathak,V.K. (2004) Azido-containing diketo acid derivatives inhibit human immunodeficiency virus type 1 integrase *in vivo* and influence the frequency of deletions at two-long-terminal-repeat-circle junctions. *J. Virol.*, **78**, 3210–3222.
25. Dash,C., Yi-Brunozzi,H.Y. and Le Grice,S.F. (2004) Two modes of HIV-1 polypurine tract cleavage are affected by introducing locked nucleic acid analogs into the (−) DNA template. *J. Biol. Chem.*, **279**, 37095–37102.
26. Schultz,S.J., Zhang,M. and Champoux,J.J. (2003) Specific cleavages by RNase H facilitate initiation of plus-strand RNA synthesis by Moloney murine leukemia virus. *J. Virol.*, **77**, 5275–5285.
27. Li,L., Olvera,J.M., Yoder,K.E., Mitchell,R.S., Butler,S.L., Lieber,M., Martin,S.L. and Bushman,F.D. (2001) Role of the non-homologous DNA end joining pathway in the early steps of retroviral infection. *EMBO J.*, **20**, 3272–3281.
28. Julias,J.G., McWilliams,M.J., Sarafianos,S.G., Alvord,W.G., Arnold,E. and Hughes,S.H. (2004) Effects of mutations in the G tract of the human immunodeficiency virus type 1 polypurine tract on virus replication and RNase H cleavage. *J. Virol.*, **78**, 13315–13324.
29. Miles,L.R., Agresta,B.E., Khan,M.B., Tang,S., Levin,J.G. and Powell,M.D. (2005) Effect of polypurine tract (PPT) mutations on human immunodeficiency virus type 1 replication: a virus with a completely randomized PPT retains low infectivity. *J. Virol.*, **79**, 6859–6867.
30. Prasad,V.R. and Goff,S.P. (1989) Linker insertion mutagenesis of human immunodeficiency virus reverse transcriptase expressed in bacteria: definition of the minimal polymerase domain. *Proc. Natl Acad. Sci. USA*, **86**, 3104–3108.
31. Prasad,V.R. (1993) Genetic analysis of Retroviral Reverse Transcriptase structure and function. In Goff,S.P. and Skalka,A.M. (eds), *Reverse Transcriptase, 1993 edn.* Cold Spring Harbor Laboratory Press, Plainview, NY, pp. 135–161.
32. Hizi,A., Hughes,S.H. and Shaharabany,M. (1990) Mutational analysis of the ribonuclease H activity from human immunodeficiency virus reverse transcriptase. *Virology*, **175**, 575–580.
33. Jacques,P.S., Wohrl,B.M., Ottmann,M., Darlix,J.L. and Le Grice,S.F. (1994) Mutating the 'primer grip' of p66 HIV-1 reverse transcriptase implicates tryptophan-229 in template-primer utilization. *J. Biol. Chem.*, **269**, 26472–26478.
34. Jacques,P.S., Wohrl,B.M., Howard,K.J. and Le Grice,S.F. (1994) Modulation of HIV-1 reverse transcriptase function in 'selectively deleted' p66/p51 heterodimers. *J. Biol. Chem.*, **269**, 1388–1393.
35. Gao,H.Q., Boyer,P.L. and Hughes,S.H. (1998) Effects of mutations in the polymerase domain on the polymerase, RNase H and strand transfer activities of human immunodeficiency virus type 1 reverse transcriptase (mb981624). *J. Mol. Biol.*, **277**, 559.
36. Julias,J.G., Boyer,P.L., McWilliams,M.J., Alvord,W.G. and Hughes,S.H. (2004) Mutations at position 184 of human immunodeficiency virus type-1 reverse transcriptase affect virus titer and viral DNA synthesis. *Virology*, **322**, 13–21.
37. Lener,D., Tanchou,V. and Darlix,J.-L. (1998) Involvement of HIV-I nucleocapsid protein in the recruitment of reverse transcriptase into nucleoprotein complexes formed *in vitro*. *J. Biol. Chem.*, **273**, 33781.
38. Hehl,E.A., Joshi,P., Kalpana,G.V. and Prasad,V.R. (2004) Interaction between human immunodeficiency virus type 1 reverse transcriptase and integrase proteins. *J. Virol.*, **78**, 5056–5067.